OXYGEN ISOTOPE SYSTEMATICS OF ALMAHATA SITTA. N. T. Kita[1], C. A. Goodrich[2], M. E. Zolensky[3], J. S. Herrin[3,4], M. H. Shaddad[5], and P. Jenniskens[6], [1]WiscSIMS, Department of Geoscience, University of Wisconsin-Madison, Madison, WI 53706 (noriko@geology.wisc.edu), [2]Planetary Science Institute, 1700 E. Ft. Lowell, Tucson, AZ 85719, [3]ARES, NASA Johnson Space Center, Houston, TX 77058, [4]ESCG Jacobs, Houston, TX 77058, [5]University of Khartoum, Khartoum 11115, Sudan, [6]SETI Institute, Mountain View, California 94043.

Introduction: The Almahata Sitta (hereafter "AHS") meteorite was derived from an impact of asteroid 2008TC_3 on Earth and is classified as an anomalous polymict ureilite [1]. More than 600 meteorite fragments have been recovered from the strewnfield [2]. Previous reports indicate that these fragments consist mainly of ureilitic materials with textures and compositions, while some fragments are found to be chondrites of a wide range of chemical classes [3-4]. Bulk oxygen three isotope analyses of ureilitic fragments from AHS [4-5] fall close to the CCAM (Carbonaceous Chondrite Anhydrous Mineral) line [6] similar to ureilites [7-8]. In order to further compare AHS with known ureilites, we performed high precision SIMS (Secondary Ion Mass Spectrometer) oxygen isotope analyses of some AHS samples.

Samples and Methods: We analyzed sections of five samples consisting of coarse-grained ureilitic lithologies (AHS #15, #36, #44, #51, #54) and one H chondrite (#25). Some of the sections were used in our previous studies [3, 9-10]. Sections of AHS #15, #25, #44 and #54 are from single chips (several mm), while AHS #36 and #51 consist of small ~mm to sub-mm sized fragments. We examined each sample using SEM. Major element compositions of olivine and pyroxene were obtained for ureilitic samples using EPMA. AHS #15 is augite-bearing ureilite that contains melt inclusions and is very similar to Hughes 009 [11]. The Mg# (=molar [Mg]/[Mg+Fe] %) of olivine and pyroxene are ~88. Twenty grains of AHS #36 are mostly monomineralic grains of olivine (Fo_{90}), low-Ca pyroxene ($En_{87}Wo_5$), and pigeonite ($En_{82}Wo_9$). AHS #44 is an olivine-pigeonite (Fo_{79}, $En_{72}Wo_{11}$) ureilite with shock-melted pyroxene rims (Fig. 1). Three mm-sized grains of AHS #51 are also monomineralic, including olivine (Fo_{90}) and pigeonite ($En_{82}Wo_9$). AHS #54 is augite bearing and has the most Mg-rich core compositions (Mg#~95) among samples we analyzed.

The SIMS oxygen isotope analyses were carried out using IMS-1280 at University of Wisconsin (WiscSIMS) using the methods similar to [12]. We used a Cs^+ ion beam with ~15μm diameter and ~5nA intensity. The external reproducibilities of $\delta^{18}O$, $\delta^{17}O$ and $\Delta^{17}O$ ($\delta^{17}O$-0.52×$\delta^{18}O$) of San Carlos olivine standard were ~0.5‰, ~0.4‰, and ~0.4‰, respectively. Multiple olivine and pyroxene standards were analyzed for matrix correction. We obtained 7-18 spot analyses on olivine and pyroxene for each sample.

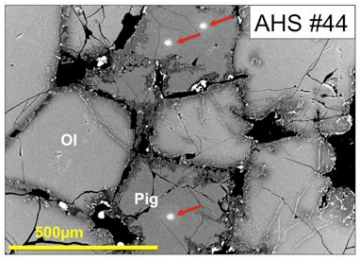

Fig. 1. AHS #44 olivine-pigeonite ureilite with coarse-grained texture. Red arrows indicate the positions of SIMS analyses.

Results and Discussion: Oxygen isotope ratios of olivine and pyroxene in five ureilitic samples are internally homogeneous within analytical uncertainties. The shock melted pyroxene and reduced olivine rim analyses from #44 do not show measurable difference from those of olivine and pyroxene core. The average oxygen isotope ratios of multiple analyses in each sample (Fig. 2) plot on the CCAM line within analytical uncertainties. These data are consistent with SIMS analyses of ureilitic clasts in polymict ureilites [13-14].

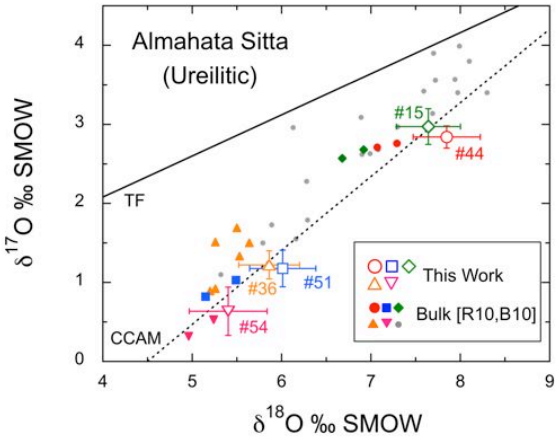

Fig. 2. Oxygen three isotope ratios of ureilitic lithologies from the AHS samples. Smaller filled symbols are analyses of bulk chips of the same AHS fragments by [5]. Gray circles (smallest) are data from [4-5] for other AHS stones.

Our data are generally consistent with the corresponding bulk data by [5], except for AHS #36 (SIMS analyses of 18 grains in this fragment were indistinguishable within analytical uncertainties). For other samples, the SIMS $\delta^{18}O$ values are slightly higher than bulk data by 0.5-1 ‰ along the mass fractionation trend. A similar difference in $\delta^{18}O$ was reported for ALHA 77257 between the SIMS analyses of [13] and the bulk analyses of [8], possibly due to contamination by Antarctic ice with low $\delta^{18}O$. In contrast, terrestrial

weathering is not significant for AHS fragments [3-4,10] and does not explain the systematic difference in $\delta^{18}O$ values between the two methods.

Data for four ureilitic fragments (except for AHS #15) show a negative correlation between Mg# and $\Delta^{17}O$ values (Fig. 3), as observed previously from the SIMS analyses of ureilitic clasts in polymict ureilites [13-14]. The $\Delta^{17}O$ values of bulk ureilites also show a similar tendency, though data show a significant scatter [7]. Similarly, bulk analyses of different stones of AHS show a large scatter [5]. Data from AHS #15 plot off the trend and are consistent with those in Hughes 009 (Mg#=87.3 [11], $\Delta^{17}O$=−1.05‰ [8]). These samples contain melt inclusions indicating that they crystallized from magma in the ureilite parent body (UPB). It is possible that UPB mantle formed as solid residues and initially had correlated Mg# and $\Delta^{17}O$ as shown in Fig. 3. AHS #15 and Hughes 009 might have formed in a large volume of magma that was created in the UPB with $\Delta^{17}O$= −1‰, in which Mg# evolved by igneous fractionation.

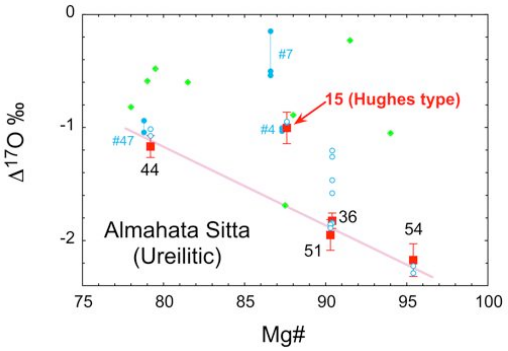

Fig. 3. Correlation between Mg# and $\Delta^{17}O$ of ureilitic samples from AHS. Red squares are data from this work. Open blue circles are bulk analyses of the same stones by [5] plotted against Mg# from this work. Bulk analyses of other AHS stones with ureilitic lithologies are shown as filled blue circles [5] and filled green circles [4].

Chondritic sample: Analyses of olivine and pyroxene from multiple chondrule phenocrysts and matrix minerals in AHS #25 show resolvable variations in the oxygen three isotope ratios. Data from a large fragment (~1mm) of a radial pyroxene (RP) chondrule and a porphyritic olivine (PO) chondrule (Fig. 4a-b) are different from the average value of four other analyses (Fig. 4c). It is possible that phenocrysts of chondrules preserved primary oxygen isotope variations, similar to those found in type 3 ordinary chondrites [11]. The average $\Delta^{17}O$ =0.65±0.17 ‰ is obtained from the four homogeneous data, which is within the range of H chondrites. Other types of chondritic materials have been identified from AHS, including E, L, and R chondrite-like samples [3-4]. These observations are similar to those reported for polymict ureilites [14-16].

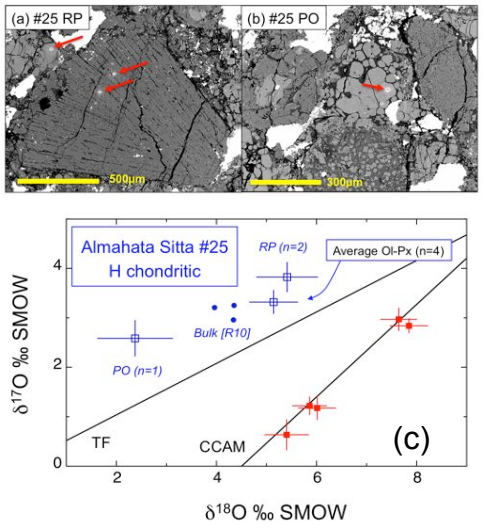

Fig. 4. AHS #25. (a-b) BSE image of chondrules. Red arrows indicate positions of SIMS analyses. (c) Oxygen isotope ratios of AHS #25 (open blue squares). Bulk chips by [5] and SIMS analyses of other AHS samples are shown as filled blue circles and filled red squares, respectively.

Conclusions: The SIMS oxygen three isotope analyses of Almahata Sitta meteorite indicate that individual fragments are internally homogeneous, like fragments of main group ureilites. The systematic trend in Mg#- $\Delta^{17}O$ from ureilitic samples and observation of various types of chondritic materials are very similar to those observed for polymict ureilites. Thus, the Almahata Sitta ureilite seems to carry source materials common to other known ureilitic meteorites.

References: [1] Jenniskens P. et al. (2009) Nature 456, 485-488. [2] Shaddad M. H. et al. (2010) *Meteoritics & Planet. Sci., 45,* 1557-1589. [3] Zolensky M. et al. (2010) *Meteoritics & Planet. Sci., 45,* 1618-1637. [4] Bishop A. et al. (2010) *Meteoritics & Planet. Sci., 45,* 1638-1656. [5] Rumble R. et al. (2010) *Meteoritics & Planet. Sci., 45,* 1765-1770. [6] Clayton R. N. et al. (1977) *EPSL, 34,* 209-224. [7] Clayton R. N. and Mayeda T. K. (1988) *GCA 52*, 1313-1318. [8] Clayton R. N. and Mayeda T. K. (1996) *GCA 60*, 1999-2017. [9] Herrin J. S. (2010) *Meteoritics & Planet. Sci., 45,* 1789-1803. [10] Goodrich C. A. et al. (2010) *Meteoritics & Planet. Sci., Suppl. 45*, A66. [11] Goodrich C. A. et al. (2001) *GCA 65*, 621–652 [12] Kita N. T. et al. (2010) *GCA 74*, 6610-6635. [13] Kita N. T. et al. (2004) *GCA 68*, 4213–4235. [14] Downes H. et al. (2008) *GCA 72*, 4825-4844. [15] Ikeda et al. (2000) *Antarctic Meteorite Res. 13*, 177–221. [16] Ikeda et al. (2003) *Antarctic Meteorite Res. 16*, 105-127.